A comparison of computational driver models using naturalistic and test-track data from cyclist-overtaking manoeuvres

Downloaded from: https://research.chalmers.se, 2025-12-05 00:13 UTC

Citation for the original published paper (version of record):
Kovaceva, J., Bärgman, J., Dozza, M. (2020). A comparison of computational driver models using naturalistic and test-track data from
cyclist-overtaking manoeuvres. Transportation Research Part F: Traffic Psychology and Behaviour, 75: 87-105. http://dx.doi.org/10.1016/j.trf.2020.09.020

N.B. When citing this work, cite the original published paper.

research.chalmers.se offers the possibility of retrieving research publications produced at Chalmers University of Technology. It covers all kind of research output: articles, dissertations, conference papers, reports etc. since 2004. research.chalmers.se is administrated and maintained by Chalmers Library

(article starts on next page)

Transportation Research Part F 75 (2020) 87–105

Contents lists available at ScienceDirect

Transportation Research Part F

journal homepage: www.elsevier.com/locate/trf

A comparison of computational driver models using naturalistic and test-track data from cyclist-overtaking manoeuvres

Jordanka Kovaceva *, Jonas Bärgman, Marco Dozza

Chalmers University of Technology, Sweden

ARTICLE INFO

Article history:
Received 22 February 2020
Received in revised form 16 September 2020
Accepted 27 September 2020
Available online 20 November 2020

Keywords:
Driver behaviour
Overtaking
Cyclist
Driver modelling
Linear program

ABSTRACT

The improvement of advanced driver assistance systems (ADAS) and their safety assessment rely on the understanding of scenario-dependent driving behaviours, such as steering to avoid collisions.

This study compares driver models that predict when a driver starts steering away to overtake a cyclist on rural roads. The comparison is among four models: a threshold model, an accumulator model, and two models inspired by a proportional-integral and proportional-integral-derivative controller. These models were tested and cross-applied using two different datasets: one from a naturalistic driving (ND) study and one from a test-track (TT) experiment. Two perceptual variables, expansion rate (the horizontal angular expansion rate of the image of the lead road user on the driver's retina) and inverse tau (the ratio between the image's expansion rate and its horizontal optical size), were tested as input to the models. A linear cost function is proposed that can obtain the optimal parameters of the models by computationally efficient linear programming.

The results show that the models based on inverse tau fitted the data better than the models that included expansion rate. In general, the models fitted the ND data reasonably well, but not as well the TT data. For the ND data, the models including an accumulative component outperformed the threshold model. For the TT data, due to the poorer fit of the models, more analysis is required to determine the merit of the models. The models fitted to TT data captured the overall pattern of steering onsets in the ND data rather well, but with a persistent bias, probably due to the drivers employing a more cautious strategy in TT.

The models compared in this paper may support the virtual safety assessment of ADAS so that driver behaviour may be considered in the design and evaluation of new safety systems.

© 2020 The Author(s). Published by Elsevier Ltd. This is an open access article under the CC BY-NC-ND license (http://creativecommons.org/licenses/by-nc-nd/4.0/).

1. Introduction

The improvement of advanced driver assistance systems (ADAS) and the assessment of new safety strategies rely on the understanding of scenario-dependent driving behaviours (Aust & Engström, 2011). Driver models used in computer simulations for the prospective safety benefit assessment of ADAS need to be expressed in mathematical (quantitative) terms (Cody & Gordon, 2007; Fruttaldo, Piccinini, Pinotti, Tadei, & Perboli, 2012; Markkula, 2015; McLaughlin, Hankey, & Dingus, 2008). A

* Corresponding author: Department of Mechanics and Maritime Sciences, Chalmers University of Technology
E-mail address: jordanka.kovaceva@chalmers.se (J. Kovaceva).

https://doi.org/10.1016/j.trf.2020.09.020
1369-8478/© 2020 The Author(s). Published by Elsevier Ltd.
This is an open access article under the CC BY-NC-ND license (http://creativecommons.org/licenses/by-nc-nd/4.0/).

counterfactual, or what-if, simulation can be used to assess safety systems by comparing what could have happened in a crash or near-crash event with and without a safety system and/or with different driver behaviours (Davis, Hourdos, Xiong, & Chatterjee, 2011).

As suggested in the review by Markkula, Benderius, Wolff, and Wahde (2012), it is not well known how proposed driver models differ, or how well they are able to reproduce the behaviour of human drivers for a given traffic scenario. The reason, according to Hamdar (2012) and Treiber and Kesting (2013), is that drivers may act differently in risky traffic conditions and scenarios.

One particularly risky scenario is when a car is approaching a cyclist from behind, in which the car driver, keeping relatively constant speed, decides to steer to overtake the cyclist. This strategy, called flying overtaking was defined by Matson and Forbes (1938) and was adapted for cyclist-overtaking by Dozza, Schindler, Bianchi-Piccinini, and Karlsson (2016). The flying strategy has been shown to be dangerous, since drivers have used it to compensate for small temporal gaps with an oncoming vehicle (Wilson & Best, 1982). Gray and Regan (2005) argue that the overtaking manoeuvre is complex because of visual judgments involved: the driver needs to simultaneously estimate time to collision (TTC) with an oncoming vehicle (to avoid head-on collision), TTC with the cyclist (to avoid rear-end collision) and time required to complete the manoeuvre based on current environment and infrastructure conditions. Consequently, the majority of overtaking crashes have been caused by inaccurate choices of timing and speed (Clarke, Ward, & Jones, 1999). Driver behaviour during overtaking has been studied with respect to different factors, such as road design, posted speed limit, presence of oncoming vehicles, drivers' and cyclists' demographics (Bella & Silvestri, 2017; Dozza et al., 2016; Feng, Bao, Hampshire, & Delp, 2018; Llorca, Angel-Domenech, Agustin-Gomez, & Garcia, 2017; Piccinini, Moretto, Zhou, & Itoh, 2018; Shackel & Parkin, 2014; Walker, 2007). On the other hand, studies that investigate the driver's decision on when to start overtaking are sparse or do not propose a driver model–with one exception: a recent study by Farah, Piccinini, Itoh, and Dozza (2019) proposes a model for the drivers' decision-making process regarding the overtaking strategy. The model, includes kinematic cues as predictors, such as vehicle speed and distance between vehicle and cyclists. However, their model is descriptive and outputs the driver's chosen strategy (accelerative or flying) only, not the driver's braking or steering initiation timing. Other studies that propose driver models for predicting brake response time in rear-end collision avoidance (Markkula et al., 2012) have used visual cues such as expansion rate $\dot{\theta}$ and inverse tau τ^{-1}. The $\dot{\theta}$ is the angular expansion rate of the lead vehicle's image falling on the retina of the driver in the following vehicle (Lamble, Laakso, & Summala, 1999). τ^{-1} is the inverse of the optically defined TTC–which assumes constant vehicle speed (Lee, 1976). In Lee (1976), drivers are assumed to start braking when τ reaches a specific threshold value. Smith, Flach, Dittman, and Stanard (2001) proposed optical angle and $\dot{\theta}$ as the criteria for driver braking in rear-end collision avoidance, while Kiefer et al. (2003) used τ^{-1} threshold. Recently, Xue, Markkula, Yan, and Merat (2018) used $\dot{\theta}$ and τ^{-1} as inputs in two types of models, threshold (Kiefer et al., 2003) and accumulator (Markkula, 2014; Markkula, Engström, Lodin, Bärgman, & Victor, 2016). Xue et al. (2018) showed that the accumulator model can explain the brake response time better than the threshold model during car-to-car rear-end collision avoidance. The brake response process has also been studied for crossing scenarios between cars and bicyclists and compared in driving simulator and test-track studies by Boda et al. (2018). However, the steering initiation timing when a driver overtakes a cyclist has not been investigated in the above studies (Boda et al., 2018; Xue et al., 2018). Driving simulators and test-tracks have been the most employed research methods for studying driver behaviour (Green, 2000). They are both performed in a strictly controlled environment and usually on predefined routes (Blaauw, 1982; Fisher, Pollatsek, & Pradhan, 2006).

Another research method that has contributed greatly to new knowledge and new conclusions concerning driving behaviour is the naturalistic driving study (Shinar, 2017). Naturalistic driving provides data on how drivers actually drive in their daily journeys, without the influence of instructions, predefined routes and preselected environments. The combination of data from test-track experiments and naturalistic driving studies has not yet been used to study driver behaviour in flying overtaking scenarios.

Drivers' decisions in overtaking manoeuvres may involve a process that generates anticipated representations from the current state of the world. The anticipation is especially important in choosing the driving actions (for the control) in normal driving situations (Hollnagel, 2006; Jagacinski & Flach, 2002). Anticipatory control has been addressed in a renowned two-level model by Donges (1978) and has been taken into account in proportional-integral-derivative (PID) control models of steering behaviour (Donges, 1999, 2016, Winner, Hakuli, Lotz, & Singer, 2; Winner et al., 2016). Another type of the control models is proportional-integral (PI) steering model by Salvucci and Gray (2004). The PID control models have been extensively used in many domains (Bennett, 1993; O'Dwyer, 2009; Rivera, Morari, & Skogestad, 1986). In this model, the proportional term is proportional to the measured signal. The integral term integrates the past values of the measured signal over time. The derivative term is an estimate of the future trend of the signal, based on its current rate of change.

Quantitative driver models (e.g., Markkula, Boer, Romano, & Merat, 2018; Salvucci, 2006; Xue et al., 2018) have been parameterised with various methods. One type of parametrisation is grid search, which approximates the problem by allowing the parameters to take discrete values and obtain a global optimum solution to the approximate problem (Xue et al., 2018). Other types of parametrisation are using heuristics that do not guarantee a global optimal solution (Salvucci, 2006), such as genetic algorithms (Markkula, 2014), or particle swarm optimisation (Benderius, Markkula, Wolff, & Wahde, 2011). Parameterisation for more complex models of decision-making that do not have analytical likelihood function (Evans, 2019), has been done by probability density approximation such as Bayesian methods (Kruschke, 2015; Lee & Lee, 2019). These methods are typically solved by searching within a vast parameter space to obtain optimal values, demanding

a large number of simulated trials to ensure an accurate estimate of the likelihood function. However, if the optimisation problems can be cast as convex programs, then computationally efficient solvers exist to find the optimal parameters, while simultaneously providing a proof that the solution is indeed a global optimum (Boyd & Vandenberghe, 2004). Convex optimisation is ubiquitous in control theory (Dorf & Bishop, 1995; Jagacinski & Flach, 2002; Levison & Cramer, 1995; Lewis & Syrmos, 1995; Sheridan & Ferrell, 1981), where the cost function is typically the minimisation of a norm of an error, and every norm is a convex function. Another example is curve fitting problems, where the cost is typically expressed as mean square error (i.e., norm two), or mean absolute error (i.e., norm one). Minimising mean absolute error, subject to affine constraints, can be accomplished by linear programming (LP), which may be seen as the simplest form of convex programming (Boyd & Vandenberghe, 2004). (Affine constraints are linear in the variables ax, and have a free term b. They are expressed as $ax + b \leqslant 0$.)

This paper employs LP to parameterise and then compare driver models that predict the time when a driver starts steering away to overtake a cyclist. These models are intended for counterfactual simulations, so that the safety benefit of ADAS, such as autonomous emergency braking and forward collision warning, can be assessed with a realistic driver behaviour. We hypothesised that the driver's steering onset timing relies on properties of an optical array and may be predicted by models in which inputs are specified in optical terms, as suggested by several studies (Lee, 1976; Yilmaz & Warren, 1995). Yilmaz and Warren (1995) suggest that the rate of change of τ can tell the driver if the current deceleration is enough to avoid a rear-end collision. In addition to their application in braking, models using visual cues have been suggested for steering control (Wann & Wilkie, 2004). In fact, the timing of steering initiation in normal avoidance may be subject to the same general principle (Kiefer, Leblanc, & Flannagan, 2005). We hypothesised that the perceptual variables may be used as excitatory or inhibitory cues to elicit steering onset. One way to explore this hypothesis is by adopting a control theory approach to the problem, which models the steering behaviour mathematically. Mathematical models are important tools for making predictions to be evaluated against experimental and real-world data and can be incorporated into computer simulations. We were motivated by the modelling in domains such as psychology and neuroscience (Gold & Shadlen, 2001, 2007; Ratcliff, 1978; Ratcliff & Smith, 2004) which have been used in driver modelling (Markkula, 2014; Ratcliff & Strayer, 2014), as well as by control theory approaches to modelling human behaviour (Jagacinski & Flach, 2002). In this paper, four models based on the different modelling paradigms, outlined above, are compared: two models based on the threshold and accumulation modelling from neuroscience (Kiefer et al., 2005; Markkula et al., 2016) and two based on control-theoretic approaches using PI and PID controllers for modelling driver behaviour. We fitted and cross-applied these models using two different datasets: one from a naturalistic driving study and one from a test-track experiment. We also propose a cost function including a mean absolute error and an additional linear term, which allows the model parameters to be optimised by a computationally efficient LP. We also investigate to what extent the regulation of perceptual variables, such as $\dot{\theta}$ and τ^{-1}, is adequate to explain drivers' steering onset time in the flying overtaking scenario.

2. Problem statement

An overtaking manoeuvre is separated into four consecutive phases, as defined by Dozza et al. (2016). In Phase 1, approaching, the driver is approaching the cyclist from behind, but both are still parallel; Phase 2, steering away, starts when the driver initiates steering away to divert from a collision course and ends when they are parallel again; in Phase 3, passing, the driver passes the cyclist, both travelling in parallel; and in Phase 4, returning, the driver has passed the cyclist and steers back into the lane in front of the cyclist: see Fig. 1.

The aim of this paper is to develop driver models that compute output signals $y_{ijk}(t)$ that can be used to indicate the onset time t_i^* when a vehicle driver steers away to overtake a cyclist. This is illustrated in Fig. 1 as the transition between Phase 1 and 2. The index $i = 1, \ldots, N_d$ represents the overtaking event, where N_d is the number of events, $j = 1, \ldots, N_{fcn}$ represents the

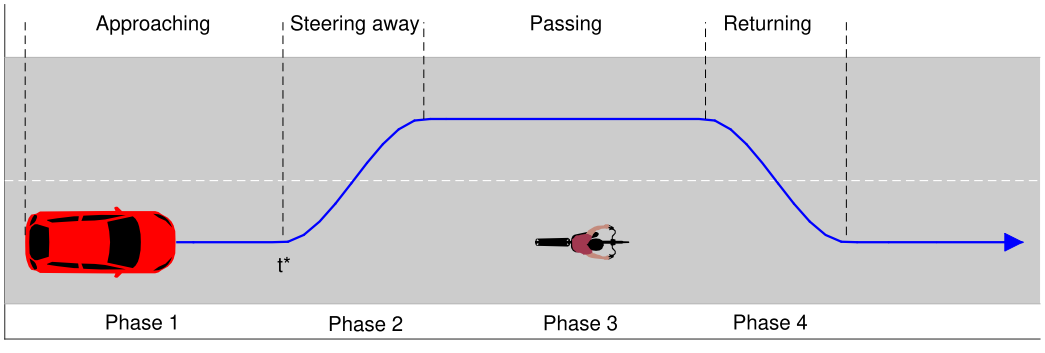

Fig. 1. The four phases as a car overtakes a cyclist; the onset time t^* is when the vehicle transits from Phase 1 to 2.

model function, where N_{fcn} is the number of functions, and $k = 1, \ldots, N_m$ represents the different combinations of signals input into the models (hereafter referred as input signals), where N_m is the number of combinations of measured signals.

The models accept an input sequence from a vector of input signals $\tilde{z}_{ik}(\eta)$. (The overline symbol tilde will be used to denote measured signals.)

Let $\tilde{\mathscr{Z}}_{ik}(t)$ be the set of values of $\tilde{z}_{ik}(\eta)$ for all input signals within a time window $\eta = [t_{0i}, t]$; i.e.,

$$\tilde{\mathscr{Z}}_{ik}(t) = \{\tilde{z}_{ik}(\eta) \,|\, \eta \in [t_{0i}, t], i = 1, \ldots, N_d, k = 1, \ldots, N_m\},$$

where t_{0i} is the time when the event starts. For more details on how t_{0i} is computed for our problem, see Section 3.2.2. We want to design functions f_j that return real-valued scalar outputs y_{ijk},

$$y_{ijk}(t) = f_j(\tilde{\mathscr{Z}}_{ik}(t), \mathbf{p}_{jk}), \quad i = 1, \ldots, N_d, j = 1, \ldots, N_{fcn}, k = 1, \ldots, N_m \tag{1}$$

given the sequence of input signals and a vector of parameters $\mathbf{p}_{jk}$. The scalar output can then be input into other systems, or be processed through an indicator function to deliver binary action to other systems; see Fig. 2. The vector of parameters $\mathbf{p}_{jk}$ is generally unknown; these could be coefficients in front of proportional, integral or other terms in f_j. The goal of this paper is for each j and k to estimate the best values of the parameters such that the error $\|y_{ijk}(t_i^*) - y_{desi}(t_i^*)\|$ between the output, y_{ijk}, obtained by the model and the desired normalised output, $y_{desi}(t_i^*) \equiv 1$, for all events i is minimised, where $\|\cdot\|$ may, in principle, denote any norm (although in this paper norm one is used, expressed as the mean absolute error). Notice that the indicator function can compare any output to a scalar threshold, but, without loss of generality, the output is here normalised such that the threshold is 1 at t_i^*. The optimal values of the parameters can then be found as the solution of the following problem

$$\min_{\mathbf{p}_{jk}} \frac{1}{N_d} \sum_{i=1}^{N_d} |f_j(\tilde{\mathscr{Z}}_{ik}(t_i^*), \mathbf{p}_{jk}) - y_{desi}(t_i^*)|, \quad j = 1, \ldots, N_{fcn}, k = 1, \ldots, N_m \tag{2a}$$

$$\text{subject to}: \ \mathbf{p}_{jk} \in \mathscr{P}_{jk} \subseteq \mathbb{R}^{N_{jk}}, \qquad j = 1, \ldots, N_{fcn}, k = 1, \ldots, N_m \tag{2b}$$

where N_{jk} is the number of parameters for model j using input signals k, and $\mathbb{R}$ is the set of real values. Problem (2) is a generalised formulation in order to check that the model is close to the target value at t_i^*. The set $\mathscr{P}_{jk}$ in (2b) can be used to, e.g., restrict the allowable values of the parameters, to restrict the model output, or impose certain properties of the functions f_j, e.g., monotonicity. Notice that if $\mathscr{P}_{jk}$ is a convex polytope and if the functions f_j are linear in their parameters $\mathbf{p}_{jk}$, then problem (2) can be stated as a LP (Boyd & Vandenberghe, 2004).

Indeed, the goal of this paper is to investigate different driver model functions f_j and find the optimal vector of parameters $\mathbf{p}_{jk}^*$ that minimises (2), for measured data $\tilde{\mathscr{Z}}_{ik}$ gathered in naturalistic settings and test-track experiments.

3. Method

3.1. Data on overtaking a cyclist

Flying overtaking events where a car driver overtakes a single bicyclist on straight rural roads were extracted from two datasets: test-track (TT) and naturalistic driving (ND) data. (In this study, the rural roads, excluding highways, have two lanes–one lane in each direction). The ND data used in this study were collected in France in the UDRIVE project (Bärgman et al., 2017). A Data Acquisition System (DAS) was installed in the vehicles, registering seven camera views (front left, front centre, front right, cabin view, cockpit view, driver face, and pedals), CAN bus data (vehicle speed, acceleration, steering wheel angle, and yaw rate), and GPS position enriched through map matching. Furthermore, the DAS recorded continuous signals from a smart camera system which included information about the presence of cyclists and their distances (lateral and longitudinal) from the vehicle. Similar vehicle data and data about the surrounding road users has been collected on a TT in Sweden. The participants drove a passenger car straight along a test-track, where they were to overtake a cyclist (represented by a dummy cyclist mounted on a high-speed platform). In a subset of the experiment an oncoming vehicle (represented by a balloon vehicle) was present. The participants in the TT experiment were instructed to keep the vehicle speed at 70km/h. A speed limiter was activated at 70km/h at the beginning of each trial, to keep the approaching speed

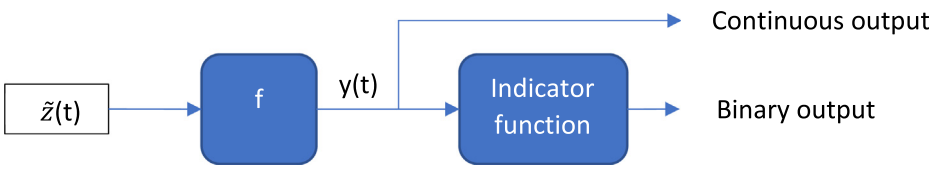

Fig. 2. The driver model is represented with function f that returns a scalar output $y(t)$. The scalar output can then be input into other systems, or processed through an indicator function to deliver binary action to other systems.

as constant as possible. The speed limiter was deactivated at 12s time-to-collision (TTC) to the cyclist throughout all trials. The time gap variable was defined as the TTC to the oncoming vehicle when the ego vehicle reached a TTC of 2s to the cyclist. The intended time gap was either 6s, 9s, or none (oncoming vehicle absent). The intended overlap value, achieved by controlling the lateral position of the cyclist in the lane, was either 0% or 50%. The participants were instructed to drive in the right lane and told that they could overtake the cyclist if they wanted to (they received no specific information about acceleration or timing constraints). The participants did not know if the trial would include an oncoming vehicle or not. The cyclist was visible when the vehicle was 200m away from the starting position of the cyclist. The cyclist's speed was 20km/h. The extracted ND data were selected to match the TT data as much as possible. For the ND events, the average vehicle speed was 70km/h (SD = 11). The average time gap to the oncoming vehicle (when present), defined as for the TT data, was 9.3s (SD = 3.8). The average cyclist's speed was 22km/h (SD = 8). The lane widths in TT and ND data were 3.7m and 3.2m (SD = 0.3), respectively. In the ND data, the start of the steering away phase (t^* in Fig. 1) was manually coded from video observations to verify that this was indeed the driver steering away to divert from the collision path with the cyclist, rather than some small steering adjustments that the driver made to stay in the lane. This confirmation was performed to be in line with the TT data, in which the steering away phase started when the steering-wheel angle last fell below -0.5degrees (negative sign indicates counter-clockwise) before the steering-wheel angle reached the peak negative amplitude of the final steering adjustment. The details of the experiment setup and data from the TT are described in Rasch et al. (2019), while the details of the identification of the overtaking manoeuvres and data from ND are described in Kovaceva, Nero, Bärgman, and Dozza (2018). The resulting datasets consisted of 83 overtaking manoeuvres from the TT study (37 without and 46 with an oncoming car) and 43 from the ND data collection (36 without and 7 with an oncoming car).

For all events, perceptual signals are calculated, including angular projection $\tilde{\theta}_i$ of the cyclist on the subject's retina, $\tilde{\theta}_i = 2\arctan(w_c/2d_i)$ and angular expansion rate $\dot{\tilde{\theta}}_i = -w_c v_i/(d_i^2 + w_c^2/4)$, where w_c is the width of the cyclist (in ND $w_c = 0.65$m, and in TT $w_c = 0.50$m), d_i is the distance between the driver's eyes and the rear of the cyclist, and v_i is the relative speed between the vehicle and the cyclist. In the ND data, the width of the cyclist was calculated as the average value of the cyclist's width as detected by the sensor, while in the TT data the actual width of the dummy bicycle was used. From these two signals we then calculated ratio $\tilde{\tau}_i = \tilde{\theta}_i/\dot{\tilde{\theta}}_i$ (Lee, 1976). The inverse of the ratio, $\tilde{\tau}_i^{-1} = 1/\tilde{\tau}_i$ has been used in response threshold models of brake onset (Kiefer et al., 2003; Maddox & Kiefer, 2012). According to these models, once $\tilde{\tau}_i^{-1}$ exceeds a given threshold, the driver brakes to avoid collision with the lead vehicle. The changes in the angular velocity during optical expansion of the lead vehicle have been shown to be a cue used to modulate braking (Yilmaz & Warren, 1995).

In this paper, as the vector of input signals we use either the expansion rate to the cyclist $\dot{\tilde{\theta}}_i$, or the inverse tau to the cyclist $\tilde{\tau}_i^{-1}$, or both $\tilde{\tau}_i^{-1}$ to the cyclist and the inverse tau to the oncoming vehicle $\tilde{\tau}_{Oi}^{-1}$, for all events i. We are focusing on the cyclist during the overtaking, and we are investigating models with either $\dot{\tilde{\theta}}_i$ or $\tilde{\tau}_i^{-1}$ to the cyclists, since these cues have not been studied before for car-to-cyclist overtaking scenario. Different cues (e.g., $\dot{\theta}, \tau$, distance, velocity, time headway, TTC) from the oncoming vehicle in overtaking have already been addressed in several studies (DeLucia, 2004; Farah et al., 2019; Gray & Regan, 2005; Levulis, DeLucia, & Jupe, 2015). Investigating models with different cues from the oncoming vehicle, in our study, would have increased the number of models even more and, with it, the complexity of the paper. To keep the paper clear and concise, we chose one of these cues, that is $\tilde{\tau}_{Oi}^{-1}$. An illustration of the $\tilde{\tau}_i^{-1}$ to the cyclist in the approaching phase for overtaking manoeuvres in the ND and TT datasets is shown in Figs. 3(a) and (b), respectively.

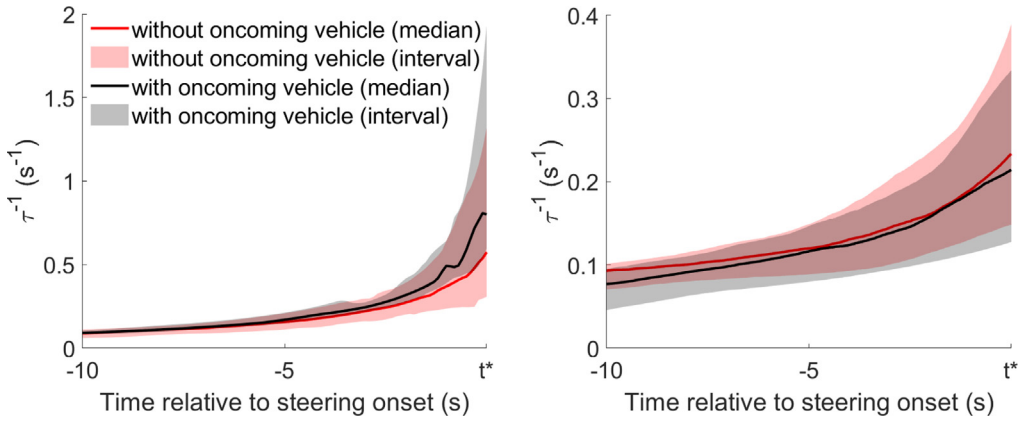

(a) τ^{-1} from naturalistic data. (b) τ^{-1} from test-track data.

Fig. 3. τ^{-1}, from all manoeuvres in naturalistic and test-track dataset, where t^* is the transition between phase 1 and 2. The manoeuvres are aligned at t^*. The solid lines show the median (50%) while the shaded region shows the confidence interval (90%) with (in black) and without (in red) oncoming vehicle. (For interpretation of the references to color in this figure legend, the reader is referred to the web version of this article.)

3.2. Driver models for steering onset time

In this section, four models are considered for predicting the steering onset time t_i^*. These include a constant threshold model, an accumulator model, and models inspired by a proportional-integral (PI) and proportional-integral-derivative (PID) control approach.

3.2.1. Constant threshold model

In the constant threshold model, once the visual cue exceeds a specific threshold, the driver will steer away from the leading vehicle. This model, usually applied to normal driving, originates from observations that drivers do not perform actions until the cues get large enough (Gordon & Magnuski, 2006; Kiefer et al., 2003; Maddox & Kiefer, 2012; Markkula et al., 2016).

Letting t_{thr} denote a constant threshold and vector $\tilde{z}_{ik}(t)$ the perceptual cues obtained from measurements, steering action is performed when

$$K^T \tilde{z}_{ik}(t) \geqslant t_{\text{thr}}$$

where K are coefficients that trade the relevance of different cues. It is clear that by dividing both sides of the inequality with t_{thr} and denoting $K_{\text{P}1k} = K/t_{\text{thr}}$, a normalised expression can be obtained

$$K_{\text{P}1k}^T \tilde{z}_{ik}(t) \geqslant 1 \tag{3}$$

where $\mathbf{p}_{1k} = K_{\text{P}1k}$ are the unknown parameters of Model 1, i.e.,

$$y_{i1k}(t) = f_1(\tilde{\mathscr{Z}}_{ik}(t), \mathbf{p}_{1k}) = K_{\text{P}1k}^T \tilde{z}_{ik}(t). \tag{4}$$

This model considers only input signals at the current instant t, thus disregarding the history that precedes t. For the vector of input signals, $N_{\text{m}} = 3$ combinations of perceptual cues are considered, i.e., the inverse tau to the cyclist $\tilde{z}_{i1} = \tilde{\tau}_i^{-1}$, or the expansion rate $\tilde{z}_{i2} = \dot{\tilde{\theta}}_i$, or both the inverse tau to the cyclist and to the oncoming vehicle $\tilde{z}_{i3} = [\tilde{\tau}_i^{-1}, \tilde{\tau}_{\text{Oi}}^{-1}]^T$. Since the model function (4) is linear in the parameters $K_{\text{P}1k}, \forall k$, the resulting problem (2) is an LP. Notice that the same model function (4) may provide three different sets of the optimal coefficients $K_{\text{P}1k}^*$, depending on the different combinations of perceptual cues, $k = 1, 2, 3$.

3.2.2. Accumulator model

The second model evaluated in this study is the evidence accumulation model which has been used in driver modelling, for example in Markkula (2014) and Ratcliff and Strayer (2014). According to this model, the drivers' action occurs after the integration of sensory evidence exceeds a given threshold. Similarly as before, the signals can be normalised such that action is triggered when $y_{ijk} \geqslant 1$. The model can then be defined as

$$y_{i2k}(t) = f_2(\tilde{\mathscr{Z}}_{ik}(t), \mathbf{p}_{2k}) = K_{\text{I}2k}^T \int_{t_{0i}}^{t} \tilde{z}_{ik}(\eta) \mathrm{d}\eta \tag{5}$$

where $\mathbf{p}_{2k} = K_{\text{I}2k}$ are the unknown parameters of Model 2. In model function (5), each signal in $\tilde{z}_{ik}$ is integrated separately.

The major difference between the accumulator model function (5) and the threshold model function (4) is that the accumulator model considers also the history of input signals that precede t. The lower bound may in theory go to minus infinity (the instant when the vehicle starts driving). However, in practice a gating function is typically invoked that saturates old input signals to zero, and preserves only recent inputs when the vehicle is close to the cyclist (Boda, Lehtonen, & Dozza, 2020; Markkula et al., 2016). Intuitively, the integration should start as soon as $\tau_i^{-1}(t_{0i})$ gets large enough and the vehicle is close to the cyclist. We choose the start value of the integral (the start of the event) to be equal to the time when $\tilde{\tau}_i^{-1}(t_{0i}) \geqslant 0.1\ \text{s}^{-1}$, which is a reference value proposed in previous studies of visual perception thresholds (Lamble et al., 1999; Summala, Lamble, & Laakso, 1998) investigating detection of and response to an approaching car assuming zero eccentricity (driver is looking at the car ahead).

It is clear that the accumulator model function (5) is more general than the threshold model function (4), since the threshold model can be obtained by disregarding all input signals in (5) except at the current sample, t.

Fig. 4 compares the accumulator model and the constant threshold model for two drivers from the TT dataset. The signals $\tau^{-1}(t)$ for the drivers are shown with red and blue curves. If the timing of the steering action is determined by evidence accumulation, then the accumulator model would respond at the stars, i.e., when the integral below the lines exceeds a certain threshold. In contrast, the threshold model would respond when the magnitude of the signals exceeds a given threshold, indicated by the circles. It can also be noted in Fig. 4 that the models respond earlier when the $\tau^{-1}(t)$ has a consistently greater rate: see the red line. Therefore, in the following we propose a fourth model that explicitly considers the time derivative (rate of change) of the perceptual cues.

3.2.3. Proportional-integral controller

The third model evaluated in this study takes into account both the proportional and integral terms of the perceptual cues

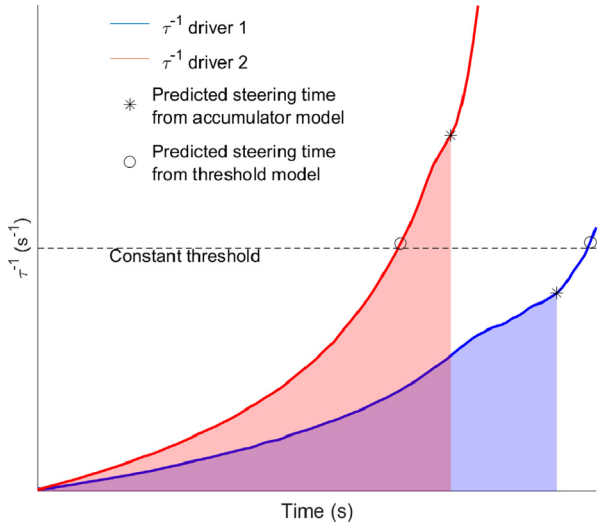

Fig. 4. The accumulator vs. threshold model. The τ^{-1} signals for two drivers on the TT overtaking a bicyclist are shown with red and blue curves. If the accumulator model is used, then the steering onset times, indicated by the star markers, are triggered when the area below the curves exceeds a certain threshold. However, the constant threshold model would indicate a steering onset time when the magnitude of the signals exceeds a certain threshold, indicated by the circle markers. (For interpretation of the references to color in this figure legend, the reader is referred to the web version of this article.)

$$y_{i3k}(t) = f_3(\tilde{\mathscr{Z}}_{ik}(t), \mathbf{p}_{3k}) = K_{\mathrm{P}3k}^T \tilde{z}_{ik}(t) + K_{\mathrm{I}3k}^T \int_{t_{0i}}^{t} \tilde{z}_{ik}(\eta)\mathrm{d}\eta \tag{6}$$

where $\mathbf{p}_{3k} = [K_{\mathrm{P}3k}^T, K_{\mathrm{I}3k}^T]^T$ are the unknown parameters of Model 3. Recall that for the overtaking scenario with an oncoming vehicle, when input signals $\tilde{z}_{i3}$ are used, model function (6) includes four parameters, two for each of the two PI gains. This model considers input signals at the current instant t and the history of the input signals at instants preceding t. In control theory, this type of PI model has been assumed to be employed by the driver for controlling the vehicle in the longitudinal direction, for example in Prokop (2001). The steering model by Salvucci and Gray (2004) is another PI driver model, consisting of a proportional gain with respect to the visual angle to two points ahead of the vehicle (near and far point on the road), and an integral gain to the near point.

3.2.4. Proportional-integral-derivative controller

Inspired by the PID regulators that are ubiquitous in control applications, the fourth model in this study takes into account the proportional, integral and derivative terms of perceptual cues

$$y_{i4k}(t) = f_4(\tilde{\mathscr{Z}}_{ik}(t), \mathbf{p}_{4k}) = K_{\mathrm{P}4k}^T \tilde{z}_{ik}(t) + K_{\mathrm{I}4k}^T \int_{t_{0i}}^{t} \tilde{z}_{ik}(\eta)\mathrm{d}\eta + K_{\mathrm{D}4k}^T \frac{\mathrm{d}\tilde{z}_{ik}(t)}{\mathrm{d}t} \tag{7}$$

where $\mathbf{p}_{4k} = [K_{\mathrm{P}4k}^T, K_{\mathrm{I}4k}^T, K_{\mathrm{D}4k}^T]^T$ are the unknown parameters of Model 4.

The PID model function (7) is more general than the previous three models, since the threshold model can be obtained by setting its parameters $K_{\mathrm{I}4k}$ and $K_{\mathrm{D}4k}$ to zero, the accumulator model by setting $K_{\mathrm{P}4k}$ and $K_{\mathrm{D}4k}$ to zero, and the PI model by setting $K_{\mathrm{D}4k}$ to zero. Recall that for the overtaking scenario with an oncoming vehicle, when input signals $\tilde{z}_{i4}$ are used, model function (7) includes six parameters, two for each of the three PID gains. The motivation to include the derivative term comes from the study by Lee (1976), which suggested that drivers' braking in rear-end scenarios is guided by the optical parameter τ and its derivative $\dot{\tau}$. Lee (1976) and Yilmaz and Warren (1995) show that drivers do not normally start to brake as soon as they see the obstacle in front; instead, they base their decision on visual information about TTC and its rate of change.

3.3. Fitting and evaluation

The model parameters were tuned separately on three training datasets: ND (N = 36) and TT (N = 37) data for manoeuvres without an oncoming vehicle and TT (N = 46) data for manoeuvres with an oncoming vehicle. A fit with ND data for the latter condition was not performed due to the low number of data points. This allowed to asses how well the models describe the data. In the tuning for all events per dataset, all-in-samples error (AE) are calculated as in (2). To evaluate the prediction performance of the models, a leave-one-out cross-validation process was performed (Hastie, Tibsherani, & Freidman, 2009; Rogers & Girolami, 2016) for each dataset and model. Within each dataset, each event was left out once while the model was optimised using the remaining events, and the left-out event was used as a test. The obtained models were then used

to predict the model output for the left out event. This was repeated N-times and a one-out-sample error (OE) was calculated as in (2) averaged for the left out events. The fitted models were also cross-applied to the TT and ND data for manoeuvres without an oncoming vehicle and ND data for manoeuvres with an oncoming vehicle, to assess model generalisability.

3.4. Augmented optimal cost function

Optimising the parameters by minimising the mean absolute error, as in (2a), may provide an output y_{ijk} that crosses the threshold $y_{desi}(t_i^*) \equiv 1$ at several time instances in $[t_{0i}, t_{fi}]$, where $t_{fi} \geqslant t_i^*$ is the final time instant of the steering away phase (i.e., the transition between Phases 2 and 3: see Fig. 1). Since the dataset includes only events with a single steering onset time t_i^*, initiatives need to be taken to encourage solutions where y_{ijk} crosses 1 only once in $[t_{0i}, t_{fi}]$, and preferably close to t_i^*. There are several ways to do this, e.g., by imposing a constraint on the parameters $\mathbf{p}_{jk}$ such that y_{ijk} is monotonically increasing, i.e.,

$$\frac{\mathrm{d}y_{ijk}(t)}{\mathrm{d}t} = \frac{\mathrm{d}f_j(\tilde{\mathscr{Z}}_{ik}(t), \mathbf{p}_{jk})}{\mathrm{d}t} \geqslant 0, \quad \forall t \in [t_{0i}, t_{fi}].$$

Another possibility applicable to the accumulator model is simply imposing $K_{ljk} \geqslant 0$, which will necessarily produce a monotonically increasing output, as long as the perceptual cues are positive within $[t_{0i}, t_{fi}]$. However, imposing such a constraint may be too restrictive for scenarios with an oncoming vehicle, where the interplay among the different perceptual cues is not straightforward. Therefore, we propose minimising an augmented cost function

$$\begin{aligned}\mathbf{p}_{jk}^* = \arg\min_{\mathbf{p}_{jk}} \frac{1}{N_\mathrm{d}} \sum_{i=1}^{N_\mathrm{d}} \left| f_j(\tilde{\mathscr{Z}}_{ik}(t_i^*), \mathbf{p}_{jk}) - y_{desi}(t_i^*) \right| + \frac{w}{t_i^* - t_{0i}} \int_{t_{0i}}^{t_i^*} \max(f_j(\tilde{\mathscr{Z}}_{ik}(t), \mathbf{p}_{jk}) - y_{desi}(t_i^*), 0)\mathrm{d}t \\ + \frac{w}{t_{fi} - t_i^*} \int_{t_i^*}^{t_{fi}} \max(y_{desi}(t_i^*) - f_j(\tilde{\mathscr{Z}}_{ik}(t), \mathbf{p}_{jk}), 0)\mathrm{d}t \end{aligned} \tag{8}$$

that includes two additional penalty terms, used only during the fitting process and disregarded during evaluation. The first term with the max function penalises output values that are greater than 1 for all time instances before t_i^*, while the second term with the max function penalises output values that are less than 1 for all instances after t_i^*. Here, w is a meta parameter that needs also to be tuned. Problem (8) is convex in $\mathbf{p}_{jk}$ for a fixed w, but it is not convex when both $\mathbf{p}_{jk}$ and w are simultaneously optimisation variables. Therefore, we commit to optimising w by a grid search, considering only a limited set of discrete values. For each grid value of w, problem (8) is solved to obtain $\mathbf{p}_{jk}^*$, which can be formulated as a standard LP (Boyd & Vandenberghe, 2004).

The penalty terms in (8) provide an additional incentive for triggering a steering action at t_i^*. If a small w is chosen, then the influence of these terms diminishes and the optimisation cost reduces to the originally stated mean absolute error.

4. Results

4.1. Model fitting and evaluation

The observed steering onset time for all manoeuvres in the TT and ND dataset is shown in Fig. 5. The model fitting results for the threshold, accumulator, PI and PID models on the manoeuvres without an oncoming vehicle with the TT dataset using $\dot{\theta}$ and τ^{-1} are shown in Table 1 and Table 2. It can be seen that all four models have lower AE when τ^{-1} is used as a perceptual cue, instead of $\dot{\theta}$. (Recall from Section 3.3 that AE is the mean absolute error between the output obtained by the model and the desired normalised output, expressed as a percentage.) Therefore, the models fitted on the ND dataset were tuned using τ^{-1} and no further results for $\dot{\theta}$ will be discussed. (Results for different weights for the models with $\dot{\theta}$ are provided in Table A.7 in Appendix A.)

The optimal parameter values for all models fitted to TT data without an oncoming vehicle are shown in Table 2, for weight $w = 1$. The differences between the OE, shown in the last column in Table 2, for the four models are marginal, which may indicate that all four models may be used to describe the TT data. (Recall from Section 3.3 that OE is the mean absolute error between the output obtained by the model and the desired normalised output, of the left-out events in the leave-one-out cross validation process. OE is expressed as a percentage.). This can also be observed from the model's output, illustrated in Fig. 6(a). The distributions are similar and centred around 1, for weight $w = 1$. For most of the drivers, the models are predicting well the steering onset time, except for the few drivers that steered away earlier (observe at Fig. 7(a) the points at a steering onset time lower than 5s). The results for the different weights from the fitting and evaluation for TT dataset without an oncoming vehicle can be seen in Table A.7 in Appendix A.

The optimal parameter values for all models for ND data without an oncoming vehicle are shown in Table 3, for weight $w = 1$. The results from the evaluation within ND, using τ^{-1} as a perceptual cue, show that for the manoeuvres without an oncoming vehicle, the PID model has less OE, two times lower than that of the threshold model (44% versus 21%) and 1% lower than the accumulator and PI models (see Table 3). The OE of the threshold model is the highest, indicated by the tail

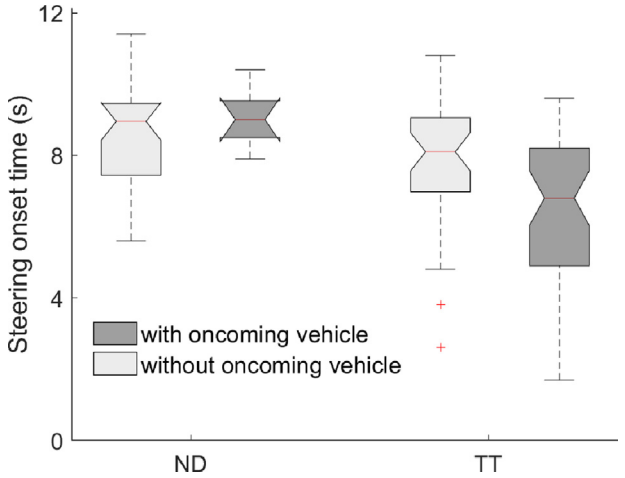

Fig. 5. The distribution of drivers' steering onset times, from start of the event, for manoeuvres in the presence (light grey) and absence (dark grey) of an oncoming vehicle. The x-axis indicates ND/TT dataset. Note: On each box, the central mark indicates the median, and the bottom and top edges of the box indicate the 25th and 75th percentiles, respectively. The whiskers extend to the most extreme data points not considered outliers, and the outliers are plotted individually using the '+' symbol. (The outliers are data points greater than $q_3 + l(q_3 - q_1)$ or less than $q_1 - l(q_3 - q_1)$, where l is the maximum whisker length, 1.5, and q_1 and q_3 are the 25th and 75th percentiles of the data, respectively.).

in the output distribution illustrated in Fig. 6(b). In contrast, the differences between the OE of the accumulator, PI and PID models are marginal. This can also be observed from the accumulator, PI and PID model output shown in Fig. 6(b), where the distributions are centred around 1, which may indicate that the three models can be used to predict the ND data (see Fig. 7(b)). The results for the different weights from the fitting and evaluation for the ND dataset are given in Table A.8 in Appendix A.

The TT drivers, in general, steered away earlier than the ND drivers. This was reflected, for the threshold model, in a different value of the parameter K_{P11} (Model 1: threshold, input signal 1: $\tilde{z} = \tau^{-1}$) for the TT (see Table 2) and ND data (see Table 3). The K_{P11} for TT is 2.6 times larger than the K_{P11} for ND, which leads to thresholds $\tau^{-1} = 1/K_{P11} = 0.26\text{s}^{-1}$ for TT and $\tau^{-1} = 1/K_{P11} = 0.70\text{s}^{-1}$ for ND. This may indicate that the TT and ND drivers use different thresholds of τ^{-1} to start steering away from the cyclist. Furthermore, in the accumulator model the value of the parameter K_{I21} for TT data is 1.6 times larger than that for ND data (see Tables 2 and 3).

The optimal parameters for all models obtained for the TT dataset, for manoeuvres with an oncoming vehicle, are shown in Table 4 for weight $w = 1$. The evaluation, regarding the manoeuvres with an oncoming vehicle in the TT dataset, gave the same OE for both the PI and PID models (Table 4), which was lower than that for the other two models (1.6 and 2.5 times lower than the OE for the threshold and accumulator models, respectively). This can also be observed in the model output in Fig. 6(c), where the distributions for the PI, PID and threshold models are centred around 1, while the distribution of the accumulator model has two peaks around 1. Fig. 7(c) shows that all models predict steering onset time later (for t^* lower than 4s) than observed.

4.2. Model cross-dataset-application

The models fitted to TT and ND dataset, shown in Tables 2 and 3, were cross-applied to the dataset not used for tuning the parameters. For example, the model fitted for the manoeuvres without an oncoming vehicle on the ND data was cross-applied on the TT data, and vice versa. The results of the cross-dataset-application are shown in Table 5. These results show that all models have large errors, which grew in the cross-dataset-applications. One reason for the larger errors on the ND dataset (both with and without an oncoming vehicle) in the cross-dataset-application could be that the models are not able to capture the behaviour of the ND drivers. The predicted onset time for the cross-applied ND data is earlier than the

Table 1
Parameters of the models (obtained from all-in-samples) and all-in-samples error (AE), and one-out-sample error (OE) from TT manoeuvres without an oncoming vehicle (the perceptual cue is $\dot{\theta}, k = 2, w = 1$).

Model	j	AE (%)	K_{Pj1} (s)	K_{Ij1} (–)	K_{Dj1} (s^2)	OE (%)
Threshold	1	53	184.60	–	–	54
Accumulator	2	44	–	79.50	–	45
PI	3	42	−39.71	95.02	–	44
PID	4	34	−665.60	283.64	273.90	35

Table 2
Parameters of the models (obtained from all-in-samples) and all-in-samples error (AE), and one-out-sample error (OE) from TT manoeuvres without an oncoming vehicle (the perceptual cue is $\tau^{-1}, k = 1, w = 1$).

Model	j	AE (%)	K_{Pj1} (s)	K_{Ij1} (–)	K_{Dj1} (s^2)	OE (%)
Threshold	1	25	3.73	–	–	26
Accumulator	2	24	–	0.82	–	25
PI	3	24	0.51	0.70	–	27
PID	4	22	5.59	-0.23	−2.48	27

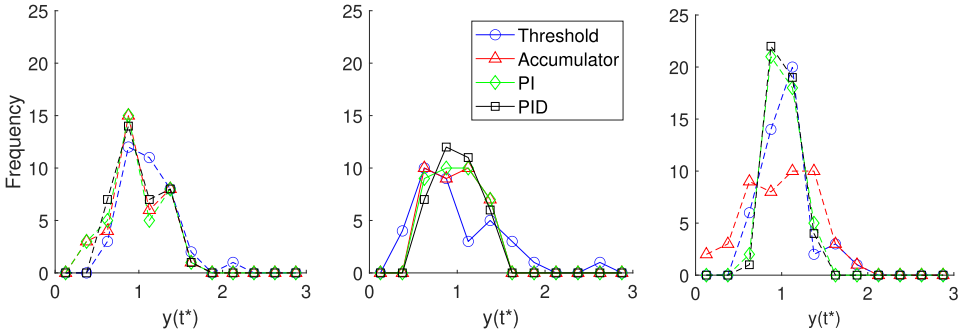

Fig. 6. Evaluation of the models with the leave-one-out cross-validation process. Distribution of the model output $y(t^*)$ for the threshold, accumulator, PI and PID models for (a) TT manoeuvres without an oncoming vehicle (N = 37); (b) ND manoeuvres without an oncoming vehicle (N = 36); (c) TT manoeuvres with an oncoming vehicle (OV) (N = 46), for weight $w = 1$.

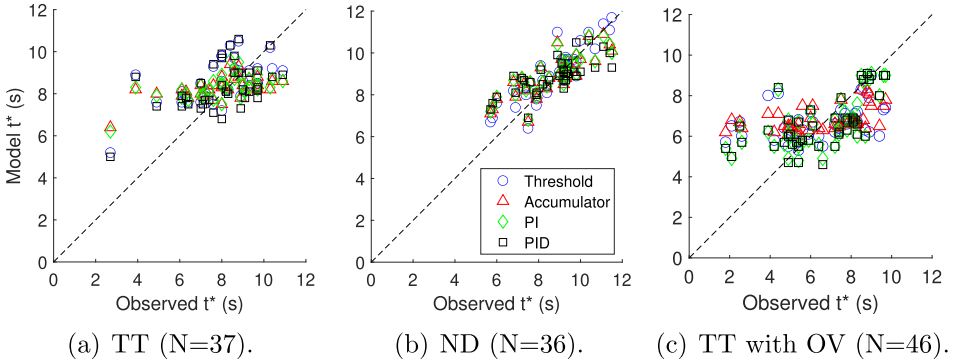

Fig. 7. Evaluation of the models with the leave-one-out cross-validation process. The predicted and observed steering onset time for the threshold, accumulator and PID models for the (a) TT manoeuvres without an oncoming vehicle (b) ND manoeuvres without an oncoming vehicle and (c) TT manoeuvres with an oncoming vehicle (OV) for $w = 1$. The dashed lines indicate $y = x$.

Table 3
Parameters of the models (obtained from all-in-samples) and all-in-samples error (AE), and one-out-sample error (OE) from ND manoeuvres without an oncoming vehicle (the perceptual cue is $\tau^{-1}, k = 1, w = 1$).

Model	j	AE (%)	K_{Pj1} (s)	K_{Ij1} (–)	K_{Dj1} (s^2)	OE (%)
Threshold	1	39	1.43	–	–	44
Accumulator	2	22	–	0.50	–	22
PI	3	21	−0.08	0.52	–	22
PID	4	20	−0.43	0.64	0.05	21

observed time, for all models fitted on the TT data, in line with what was noted above about earlier steering onsets in the TT data; see Fig. 8(a) and (b). This can also be seen in the models' output, illustrated in Fig. 9(a): the distributions are centred around 2, instead of 1. The opposite is observed for the models that are fitted on ND data without an oncoming vehicle and cross-applied on the TT data without an oncoming vehicle: see Fig. 8(c). For all four models, the predicted onset time is later

Table 4
Parameters of the models (obtained from all-in-samples) and all-in-samples error (AE), and one-out-sample error (OE) from TT manoeuvres with an oncoming vehicle (the perceptual cue is $\tau^{-1}, k = 3, w = 1$).

Model	j	AE (%)	K_{Pj3} (s)	K_{Ij3} (–)	K_{Dj3} (s^2)	K_{Pj3} (s)	K_{Ij3} (–)	K_{Dj3} (s^2)	OE (%)
Threshold	1	22	3.39	–	–	3.84	–	–	22
Accumulator	2	34	–	1.19	–	–	−0.44	–	36
PI	3	13	0.64	0.80	–	18.05	−3.40	–	14
PID	4	13	1.45	0.61	−0.89	16.46	−2.90	−2.09	14

Table 5
Cross-dataset-application of the fitted models. The all-in-samples error (AE) in the first two columns is for the models fitted on TT but cross-applied to ND data, and the other way around for the last column.

Model	j	ND without OV AE (%)	ND with OV AE (%)	TT without OV AE (%)
Threshold	1	157	426	63
Accumulator	2	62	126	41
PI	3	74	518	39
PID	4	115	299	34

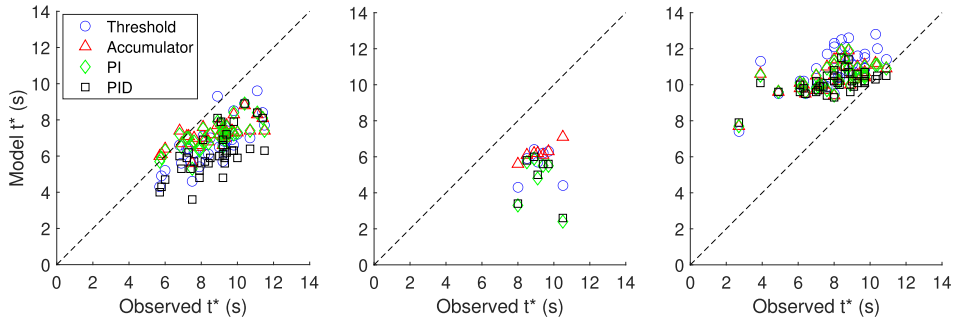

Fig. 8. Cross-dataset-application of the fitted models. The predicted and the observed steering onset time for the threshold, accumulator, PI and PID models for the (a) ND manoeuvres without oncoming vehicle (b) ND with oncoming vehicle (OV) and (c) TT manoeuvres without oncoming vehicle for $w = 1$.

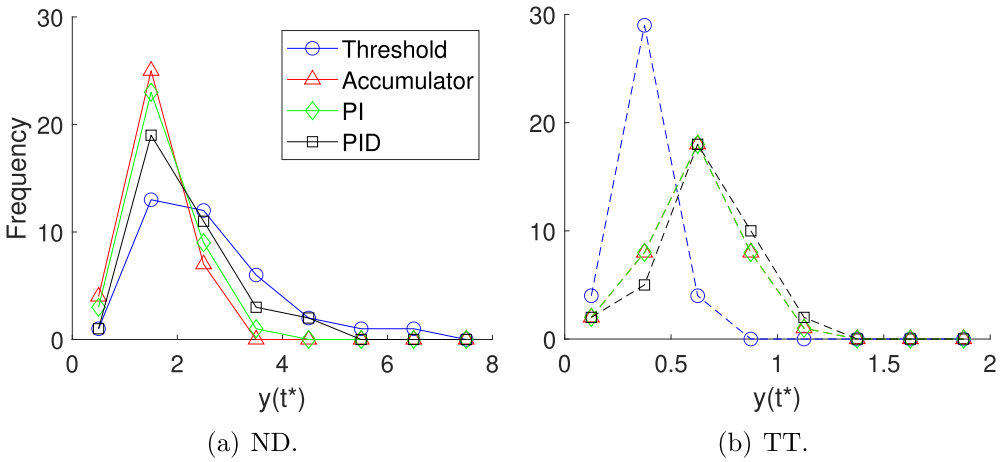

Fig. 9. Cross-dataset-application of the fitted models. Distribution of the model output $y(t^*)$ for the threshold, accumulator, PI and PID models cross-applied on (a) ND manoeuvres without oncoming vehicle (N = 36), (b) TT manoeuvres without oncoming vehicle (N = 37), for weight $w = 1$.

than the observed. Regardless of the model, the distributions of the model output are shifted to values lower than 1, as illustrated in Fig. 9(b).

5. Discussion

5.1. Driver models and perceptual cues

The expansion rate $\dot{\theta}$ and inverse tau τ^{-1} have been used in previous studies to quantify situation urgency and the need for driver braking in rear-end scenarios (Lamble et al., 1999; Maddox & Kiefer, 2012; Markkula, 2015). However, the comparison of the measures for overtaking scenario in which drivers steer instead of brake, have not been performed before. In this study, the models based on the τ^{-1} fitted the data better than the models that included $\dot{\theta}$, according to the values of the cost function (shown in Table 2 and Table 1). This finding is in line with a recent study on brake response timing by Xue et al. (2018), which found that the drivers make use of the visual cues that are more similar to τ^{-1} than $\dot{\theta}$, which may indicate that the drivers are responding to higher order of variable (higher order optical primitive e.g., τ^{-1}) and could be indifferent to changes in the underlying variables (lower order primitives e.g., angle θ and angular rate $\dot{\theta}$) that leave the higher order variable the same (Jagacinski & Flach, 2002).

The models were not able to capture the responses that the drivers performed when the cue τ^{-1} was weak ($\tau^{-1} \leqslant 0.15\ s^{-}1$) in the TT dataset (observe the points at steering onset time lower than 5s in Fig. 7(a)). In these cases, the drivers initiated the steering away faster than the models predicted. This indicates that the drivers might be using some other sensory evidence to initiate the steering when the τ^{-1} cue is weak (DeLucia, 2004; Levulis et al., 2015). Furthermore, the drives may have anticipated their manoeuvre in response to the oncoming vehicle in the TT trials because of repetition. In fact, in the TT experiment, the highly repetitive task might have nourished some expectations about the oncoming vehicle and facilitated an anticipatory behaviour. Such an anticipation might have presumably led to earlier steering onset times for the TT dataset but was not explicitly taken into account in the models considered in this study.

The drivers in the two datasets, ND and TT, were different with respect to the threshold at which they initiate the steering based on the τ^{-1} cue. The threshold values obtained show that τ^{-1} threshold in ND data was 2.6 times higher than in TT data. This shows that the drivers in the TT dataset drove in a more cautious and controlled mode (Green, 2000) or made earlier decision to show a safe behaviour to the experimenters. The ND drivers drive closer to cyclists and initiate the steering at higher τ^{-1} (lower TTC), than TT drivers. One possible reason is that the TT drivers may have anticipated the oncoming car due to multiple repetitions of the experiment while in ND there are no repetitions. They may have also acted more conservatively than they would in everyday routine driving. Furthermore, we need to acknowledge that some of the differences may originate from the country-specific driving style, since the TT data were collected in Sweden and the ND data in France. The ND data in our study was part of the UDRIVE project which have observed some cross-country differences in the driving style (Bärgman et al., 2017). When the models were cross-applied between datasets, the difference in the steering onset time between TT and ND data, was observed as a persistent bias in the predicted onset time (either earlier or later compared to the observed onset in each dataset).

Through the comparison of the threshold, accumulator, PI and PID models, we investigated which terms (proportional, integral and derivative) are adequate to be included in the models that indicate when a vehicle driver steers away to overtake the cyclist. For the ND data without an oncoming vehicle, the differences in the OE results for the accumulator, PI and PID models were marginal indicating that the integral term is needed for predicting the steering onset. However, the accumulator model might be preferred to be used for example in counterfactual simulations because it had similar OE as PI and PID but it is less complex than the other two models. Furthermore, there are indications that the derivative term, or the rate of change of τ^{-1}, may provide additional value since the decision to steer away might be comparable to the decision to brake in a rear-end situation (Lee, 1976; Yilmaz & Warren, 1995) (because, before steering away, the driver is on a rear-end collision course with the cyclist). Thus the decision to steer away might also depend on τ^{-1} and its rate of change. However, further analysis is needed to confirm this.

On the other hand, for the TT data without an oncoming vehicle, all models gave similar OE which made it hard to decide which model is best. The drivers on TT might have used other cues (e.g., in the environment) to make the decision (DeLucia, 2004) than the ones taken into account in this study. The experiment on the TT was repetitive, making the drivers develop expectations during the experiment and this may have induced an anticipatory behaviour.

5.2. Cost function

The definition of cost functions and the development of methods for obtaining the model parameters is a non-trivial task in the design of driver models. Another issue that arises when the models include many parameters is the computational time needed for finding their optimal values. The LP used here provides a computationally efficient way to find the parameters and ensures a global minimum solution for our definition of the error and our choice of the cost function defined in (8). In a matter of seconds, it allowed us to test four different quantitative models with a maximum of six parameters on two datasets and different input signals, for the purpose of ADAS safety assessment in the early stage of ADAS development.

The weight in the cost function allows further fine-tuning the desired behaviour (crossing the threshold only once), by penalising values that are greater than the threshold before t^*, or less than the threshold after t^*. For two monotonically increasing functions with the same error at t^*, the weighted terms will favour the one that is steeper near t^*. An example of the accumulator model, applied to three events from TT data without an oncoming vehicle, is shown in Fig. 10. We can see that the accumulator model shows poor fit for two of the events, where the model predicts either later (event 1, OE is 35%) or earlier (event 3, OE is 18%) steering onset time than the observed. For event 2, the accumulator model is close to 1 (OE is 1%) for the observed steering onset time (which means that the modelled and observed steering onset times are close). The use of the augmented cost function (8) allowed us to investigate the optimal values of the parameters without imposing constraints on the parameters that may unnecessarily reduce the search space. This is especially relevant for the manoeuvres with an oncoming vehicle, where the interplay among the different perceptual cues is not straightforward. For example, the parameters obtained for the accumulator model suggest that the driver may use the τ^{-1} of the cyclist as an excitatory cue ($K_{I23} > 0$) to initiate steering, and the τ^{-1} of the oncoming vehicle as an inhibitory cue ($K_{I23} < 0$) against the steering. It may be that drivers have different schemata (Nashner & Cordo, 2004) and comfort zone boundaries when another (oncoming) vehicle is involved (Summala, 2007; Summala et al., 1998). In fact, previous studies have found that drivers change their comfort zone boundaries when an oncoming vehicle is present (Dozza et al., 2016; Kovaceva et al., 2018; Rasch et al., 2019).

5.3. Limitations and future work

In this study, we have not investigated individual driver differences or intra-driver variability in a rigorous manner (due to the small datasets), but a single set of estimated values was used for all model parameters. To keep analysis consistent between the two datasets, the intra-driver variability was not investigated, since the two datasets are different in nature. That is, in the TT dataset there were repetitions per driver, while in the ND dataset there were not. Therefore, future studies should consider driver variability and its effect and sensitivity with respect to parameter fitting and model performance.

The observed lack of alignment of the model and the observed drivers' steering onset, with the $y = x$ line (Fig. 7(a)), as well as the variability in model parameters between different datasets, may be due to driver anticipation which was not taken into account in the models considered in this study, or a cognitive state that we cannot measure (and is therefore not included in the model) (Boer, 1999). The analysis in this paper compared different models fitted to normal everyday driving situations, in which the drivers see the cyclist and keep their eyes on the road. This study did not attempt to develop (or fit) models to safety-critical situations, such as near-crashes (when the driver's response may be late due to distraction or fatigue). Studies have shown that drivers' responses can differ from normal everyday driving when they respond to critical situations (Markkula, 2015). Further, the models' inability to account for an inattentive driver may be problematic for counterfactual simulations, since inattentive drivers have been part of the simulations (Bärgman et al., 2017). However, the models evaluated in this paper could still be relevant for threat-assessment algorithms for ADAS activation. For example, in an overtaking manoeuvre, the model may predict that an attentive driver had already started to steer away when the actual driver did not, the ADAS could then act on this mismatch, thus supporting an impaired driver in avoiding a collision (Hosseini, Murgovski, de Campos, & Sjøberg, 2016; Sjöberg, Coelingh, Ali, Brännström, & Falcone, 2010). In other words, ADAS should act when there is a mismatch between what the driver model predicts and what the driver does. In order to reduce the discrepancies between the two datasets, future studies may mix the data from TT and ND, both for fitting and cross-dataset-application.

In this study we have considered only the flying overtaking strategy, in which the driver performs a steering action to initiate the overtaking and keeps an almost constant speed. That is, the steering timing in the flying strategy is studied,

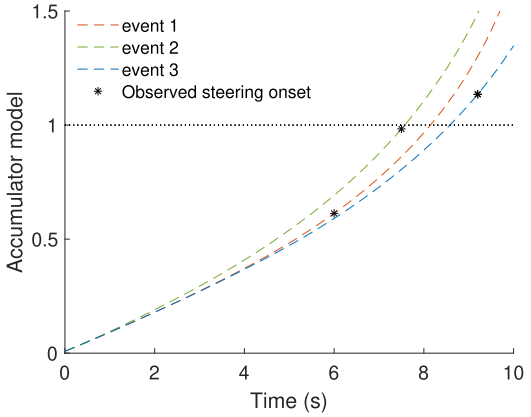

Fig. 10. The accumulator model applied to three TT events without an oncoming vehicle.

not the drivers' choice of overtaking strategy. In a subsequent step, improved driver models will be needed that consider different overtaking strategies (e.g., accelerative and flying), for which the driver has to decide between alternative actions: braking or steering. Future work should include a driver model that predicts brake pedal pressure and steering angle, and not just the timing when these actions occur (see e.g., Boda et al. (2020) and Salvucci & Gray (2004)). Furthermore, the gating value of 0.1 s^{-1} that was used to indicate the start of the overtaking event can also be regarded as a parameter to be tuned, as in Boda et al. (2020), for example.

The parameter optimisation of the models was carried out using the data pertaining to drivers' steering away from the cyclist when the ego vehicle had an average approaching speed of 70 km/h. However, we have not tested whether the models are valid for other speeds. Due to the relatively small datasets, if more parameters had been considered (than in the current models), the result may have been poor model generalisation. In the future, larger datasets that include a variety of situations, e.g., drivers with different approaching speeds or those who failed to avoid the cyclist (ending in a crash), should also be considered. In this study, only overtaking events when a car driver overtakes a single bicyclist on a straight rural road were included. There are other quantitative models that could be compared which include multiple cyclists and capture more of the steering process (Hildreth, Beusmans, Royden, & Boer, 2000; Salvucci, 2006). Furthermore, only two signals were used as input to the models: $\dot{\theta}$ and τ^{-1}, based on the theory developed by Lee (1976) and several following studies (Markkula et al., 2016; Xue et al., 2018). In future work, a combination of these visual cues and other input (derived from visual cues) could be considered, such as longitudinal looming (Boda et al., 2020). Additional inputs to the models which take into account the road profile, curvature or gradient (Lappi, 2014; Lehtonen, Lappi, & Summala, 2012) could also be included.

Our method requires a very short computation time but it does not include a model of the variance of response time within the accumulator models, for example in terms of noise (Ratcliff, Smith, Brown, & Gail, 2016). Future work should investigate the implications of this methodological limitation and reflect on the benefits of fast model fit versus the drawbacks from not including, for example, accumulation noise. Furthermore, the models were tested with one cost function, and constraints were not imposed on the parameters. In future, other cost functions, constraints on the parameters or other parameter optimisation methods could be compared by defining different functions (e.g., polynomial, exponential, trigonometric), different number of parameters (e.g., 2nd and 3rd order polynomial), and more input signals.

6. Conclusion

In this paper four types of models were compared that compute an output value indicating when a car driver starts steering away to overtake a cyclist in the flying overtaking strategy. A comparison of quantitative driver models for the cyclist-overtaking scenario on two datasets, test-track and naturalistic driving data, has not been performed before. This paper describes a method for optimising model parameters that can be used to fit data from any dataset. The method, applied to both test-track and naturalistic driving data, provides a computationally efficient way to find the parameters and ensures that we obtain a global minimum solution for our definition of error and our choice of cost function.

The models based on τ^{-1} fitted the data better than the models that included $\dot{\theta}$, according to the values of the cost function. This finding may be taken into consideration when deciding which measured signals could be included as input to more comprehensive driver models that address all phases of the overtaking manoeuvres.

The models with an accumulative component were superior to the threshold model for the manoeuvres without an oncoming vehicle in the ND data. The same could not be confirmed for the TT data for which the models showed poorer model fit, possibly due to some drivers initiating early steering onset due to anticipation and caution. The models fitted to TT data captured the overall pattern of steering onsets in the ND data rather well, but with a persistent bias, seemingly due to the TT drivers employing a more cautious/anticipatory strategy.

The drivers seem to use τ^{-1} from the cyclist as an excitatory cue to initiate steering and τ^{-1} from the oncoming vehicle as an inhibitory cue for the same action. However, it remains to be confirmed if the rate of change of τ^{-1} (the derivative term in PID) is used by the drivers in these situations, since the small number of manoeuvres with an oncoming vehicle in the ND dataset did not allow fitting the models. The models cast light on the selection of suitable driver models to enable virtual assessment of new ADAS. Future work may focus on using larger and more diverse datasets and investigating more advanced models, before including them in counterfactual simulations.

CRediT authorship contribution statement

Jordanka Kovaceva: Software, Formal analysis, Data curation, Methodology, Writing - original draft, Writing - review & editing, Visualization, Validation. **Jonas Bärgman:** Conceptualization, Methodology, Writing - review & editing, Supervision. **Marco Dozza:** Conceptualization, Methodology, Writing - review & editing, Supervision, Project administration, Funding acquisition.

Declaration of Competing Interest

The authors declare that they have no known competing financial interests or personal relationships that could have appeared to influence the work reported in this paper.

Acknowledgements

The authors would like to thank Christian-Nils Boda, Prateek Thalya and Alessia Knauss for test-track data collection. Additionally, the authors acknowledge Kristina Mayberry for language revisions. The study was supported by the MICA project (Ref. No. 2017-05522) sponsored by Vinnova, within FFI program (strategic vehicle research and innovation), Sweden. The test-track data used in this publication were collected as part of the DIV project sponsored by Toyota Motor Europe, Belgium, Veoneer, Sweden and Autoliv Research, Sweden. The naturalistic driving data were collected in the European project UDRIVE (GA No. 314050).

Appendix A. Parameter values

Tables A.6–A.11

Table A.6
Parameters of the models and AE, and evaluation with leave-one-out cross-validation process, from TT manoeuvres without an oncoming vehicle (the perceptual cue is $\dot{\theta}, k = 2$). The weighted error is given in (8).

Model	j	w	Weighted error (%)	AE (%)	K_{Pj2} (s/rad)	K_{Ij2} (1/rad)	K_{Dj2} (s^2/rad)	OE (%)
Threshold	1	0.2	54	52	158.11	–	–	53
Accumulator	2	0.2	45	44	–	77.18	–	45
PI	3	0.2	43	42	−41.67	95.57	–	43
PID	4	0.2	34	31	−829.17	335.89	326.88	33
Threshold	1	0.5	57	52	175.12	–	–	53
Accumulator	2	0.5	48	44	–	79.21	–	45
PI	3	0.5	46	42	−40.02	94.94	–	43
PID	4	0.5	37	33	−856.55	340.68	359.50	34
Threshold	1	1	62	53	184.60	–	–	54
Accumulator	2	1	51	44	–	79.50	–	45
PI	3	1	49	42	−39.71	95.02	–	44
PID	4	1	41	34	−665.60	283.64	273.90	35
Threshold	1	2	71	54	202.81	–	–	55
Accumulator	2	2	58	45	–	83.93	–	47
PI	3	2	56	43	−41.77	100.26	–	44
PID	4	2	48	35	−621.54	275.54	250.33	36
Threshold	1	5	94	58	231.59	–	–	59
Accumulator	2	5	78	47	–	93.69	–	48
PI	3	5	75	45	−45.84	110.31	–	46
PID	4	5	67	37	−535.77	257.73	198.98	38

Table A.7
Parameters of the models and AE, and evaluation with leave-one-out cross-validation process from TT manoeuvres without an oncoming vehicle (the perceptual cue is $\tau^{-1}, k = 1$). The weighted error is given in (8).

Model	j	w	Weighted error (%)	AE (%)	K_{Pj1} (s)	K_{Ij1} (–)	K_{Dj1} (s^2)	OE (%)
Threshold	1	0.2	26	25	3.64	–	–	27
Accumulator	2	0.2	25	24	–	0.81	–	26
PI	3	0.2	25	24	−0.98	1.01	–	28
PID	4	0.2	22	22	5.06	−0.15	−2.49	28
Threshold	1	0.5	27	25	3.64	-	-	26
Accumulator	2	0.5	26	24	–	0.81	–	25
PI	3	0.5	26	24	0.36	0.73	–	27
PID	4	0.5	24	22	4.97	−0.14	−2.30	27
Threshold	1	1	28	25	3.73	–	–	26
Accumulator	2	1	28	24	–	0.82	–	25
PI	3	1	28	24	0.51	0.70	–	27
PID	4	1	25	22	5.59	−0.23	−2.48	27
Threshold	1	2	31	26	3.92	–	–	27
Accumulator	2	2	31	24	–	0.82	–	25
PI	3	2	31	24	1.11	0.58	–	28
PID	4	2	28	22	6.21	−0.32	−2.70	28
Threshold	1	5	41	26	4.06	–	–	27
Accumulator	2	5	41	25	–	0.83	–	26
PI	3	5	39	25	2.62	0.29	–	28
PID	4	5	35	23	5.79	−0.23	−2.54	28

Table A.8
Parameters of the models and AE, and evaluation with leave-one-out cross-validation process from ND manoeuvres without an oncoming vehicle (the perceptual cue is $\tau^{-1}, k = 1$). The weighted error is given in (8).

Model	j	w	Weighted error (%)	AE (%)	K_{Pj1} (s)	K_{Ij1} (–)	K_{Dj1} (s^2)	OE (%)
Threshold	1	0.2	40	39	1.37	–	–	44
Accumulator	2	0.2	23	22	–	0.49	–	22
PI	3	0.2	22	21	−0.09	0.51	–	22
PID	4	0.2	21	20	−0.75	0.72	0.11	21
Threshold	1	0.5	42	39	1.41	–	–	44
Accumulator	2	0.5	24	22	–	0.49	–	22
PI	3	0.5	23	21	−0.09	0.52	–	22
PID	4	0.5	22	20	−0.51	0.66	0.07	21
Threshold	1	1	44	39	1.43	–	–	44
Accumulator	2	1	25	22	–	0.50	–	22
PI	3	1	25	21	−0.08	0.52	–	22
PID	4	1	24	20	−0.43	0.64	0.05	21
Threshold	1	2	48	40	1.54	–	–	45
Accumulator	2	2	29	22	–	0.50	–	23
PI	3	2	28	22	−0.09	0.54	–	23
PID	4	2	27	21	−0.38	0.63	0.04	22
Threshold	1	5	59	42	1.66	–	–	46
Accumulator	2	5	38	24	–	0.53	–	25
PI	3	5	37	22	−0.09	0.55	–	24
PID	4	5	37	22	−0.36	0.65	0.03	23

Table A.9
Parameters of the models and AE, and evaluation with leave-one-out cross-validation process from TT manoeuvres with an oncoming vehicle (the perceptual cues are τ^{-1} to the cyclist and τ^{-1} to the oncoming vehicle, $k = 3$).

Model	j	w	Weighted error (%)	AE (%)	K_{Pj3} (s)	K_{Ij3} (–)	K_{Dj3} (s^2)	K_{Pj3} (s)	K_{Ij3} (–)	K_{Dj3} (s^2)	OE (%)
Threshold	1	0.2	23	21	3.38	–	–	3.87	–	–	22
Accumulator	2	0.2	36	34	–	1.18	–	–	−0.42	–	36
PI	3	0.2	15	13	0.64	0.80	–	18.05	−3.40	–	14
PID	4	0.2	15	13	1.45	0.60	−0.89	16.53	−2.90	−2.19	14
Threshold	1	0.5	24	22	3.39	–	–	3.84	–	–	22
Accumulator	2	0.5	37	34	–	1.18	–	–	−0.43	–	36
PI	3	0.5	16	13	0.64	0.80	–	18.05	−3.40	–	14
PID	4	0.5	16	13	1.45	0.61	−0.89	16.48	−2.90	−2.11	14
Threshold	1	1	25	22	3.39	–	–	3.84	–	–	22
Accumulator	2	1	38	34	–	1.19	–	–	−0.44	–	36
PI	3	1	17	13	0.64	0.80	–	18.05	−3.40	–	14
PID	4	1	17	13	1.45	0.61	−0.89	16.46	−2.90	−2.09	14
Threshold	1	2	26	22	3.39	–	–	3.84	–	–	22
Accumulator	2	2	39	34	–	1.19	–	–	−0.44	–	36
PI	3	2	18	13	0.64	0.80	–	18.05	−3.40	–	14
PID	4	2	18	13	1.45	0.61	−0.89	16.46	−2.90	−2.09	14
Threshold	1	5	27	22	3.39	–	–	3.84	–	–	22
Accumulator	2	5	41	34	–	1.19	–	–	−0.44	–	36
PI	3	5	20	13	0.64	0.80	–	18.05	−3.40	–	14
PID	4	5	20	13	1.45	0.61	−0.89	16.46	−2.90	−2.09	14

Table A.10
Cross-dataset-application of the fitted models on the manoeuvres without an oncoming vehicle. The AE in the first column is for the models fitted on ND but cross-applied to TT data, and the other way around for the last column.

Model	j	*w*	TT AE (%)	ND AE (%)
Threshold	1	0.2	65	151
Accumulator	2	0.2	42	61
PI	3	0.2	41	69
PID	4	0.2	33	96
Threshold	1	0.5	64	151
Accumulator	2	0.5	41	61
PI	3	0.5	40	70
PID	4	0.5	34	101
Threshold	1	1	63	157
Accumulator	2	1	41	62
PI	3	1	39	74
PID	4	1	34	115
Threshold	1	2	60	170
Accumulator	2	2	40	62
PI	3	2	37	90
PID	4	2	35	130
Threshold	1	5	57	179
Accumulator	2	5	37	65
PI	3	5	36	120
PID	4	5	33	126

Table A.11
Cross-dataset-application of the fitted models on the manoeuvres with an oncoming vehicle. The AE is for the models fitted on TT but cross-applied to ND data.

Model	j	*w*	AE (%)
Threshold	1	0.2	425
Accumulator	2	0.2	123
PI	3	0.2	517
PID	4	0.2	293
Threshold	1	0.5	426
Accumulator	2	0.5	124
PI	3	0.5	518
PID	4	0.5	297
Threshold	1	1	426
Accumulator	2	1	126
PI	3	1	518
PID	4	1	299
Threshold	1	2	426
Accumulator	2	2	126
PI	3	2	518
PID	4	2	299
Threshold	1	5	426
Accumulator	2	5	126
PI	3	5	518
PID	4	5	299

References

Aust, M. L., & Engström, J. (2011). A conceptual framework for requirement specification and evaluation of active safety functions. *Theoretical Issues in Ergonomics Science, 12*, 44–65. https://doi.org/10.1080/14639220903470213.

Bärgman, J., van Nes, N., Christoph, M., Jansen, R., Heijne, V., Dotzauer, M., & Carsten, O. (2017). UDrive Deliverable D41.1: The UDrive Dataset and Key Analysis Results. Technical Report. EU. UDRIVE. Deliverable D.41.1.

Bella, F., & Silvestri, M. (2017). Interaction driver-bicyclist on rural roads: Effects of cross-sections and road geometric elements. *Accident Analysis and Prevention, 102*, 191–201. https://doi.org/10.1016/j.aap.2017.03.008.

Benderius, O., Markkula, G., Wolff, K., & Wahde, M. (2011). A simulation environment for analysis and optimization of driver models. In V. G. Duffy (Ed.), *Digital Human Modeling* (pp. 453–462). Heidelberg: Springer, Berlin.

Bennett, S. (1993). Development of the PID controller. *IEEE Control Systems, 13*, 58–62. https://doi.org/10.1109/37.248006. https://ieeexplore.ieee.org/document/248006/.

Blaauw, G. J. (1982). Driving experience and task demands in simulator and instrumented car: A validation study. *Human Factors, 24*, 473–486. https://doi.org/10.1177/001872088202400408.
Boda, C., Lehtonen, E., & Dozza, M. (2020). A computational driver model to predict driver control at unsignalised intersections. *IEEE Access, 8*, 104619–104631.
Boda, C. N., Dozza, M., Bohman, K., Thalya, P., Larsson, A., & Lubbe, N. (2018). Modelling how drivers respond to a bicyclist crossing their path at an intersection: How do test track and driving simulator compare? *Accident Analysis and Prevention, 111*, 238–250. https://doi.org/10.1016/j.aap.2017.11.032.
Boer, E. R. (1999). Car following from the driver's perspective. *Transportation Research Part F: Traffic Psychology and Behaviour, 2*, 201–206. https://doi.org/10.1016/S1369-8478(00)00007-3.
Boyd, S., & Vandenberghe, L. (2004). *Convex optimization* (first ed.). London: Cambridge University Press.
Clarke, D. D., Ward, P. J., & Jones, J. (1999). Processes and countermeasures in overtaking road accidents. *Ergonomics, 42*, 846–867. https://doi.org/10.1080/001401399185333.
Cody, D., & Gordon, T. (2007). Trb workshop on driver models: A step towards a comprehensive model of driving? In P. C. Cacciabue (Ed.), *Modelling Driver Behaviour in Automotive Environments* (pp. 26–42). London: Springer. https://doi.org/10.1007/978-1-84628-618-6.
Davis, G. A., Hourdos, J., Xiong, H., & Chatterjee, I. (2011). Outline for a causal model of traffic conflicts and crashes. *Accident Analysis and Prevention, 43*, 1907–1919. https://doi.org/10.1016/j.aap.2011.05.001.
DeLucia, P. R. (2004). Chapter 11 multiple sources of information influence time-to-contact judgments: Do heuristics accommodate limits in sensory and cognitive processes? In H. Hecht, G. J. Savelsburgh (Eds.), *Time-to-Contact. Advances in Psychology* (Vol. 135, pp. 243–285). North-Holland. doi: 10.1016/S0166-4115(04)80013-X.
Donges, E. (1978). A two level model of driver steering behavior. *Human Factors, 20*, 691–707.
Donges, E. (1999). A conceptual framework for active safety in road traffic. *Vehicle System Dynamics, 32*, 113–128. https://doi.org/10.1076/vesd.32.2.113.2089.
Donges, E. (chap. 2). Driver behavior models. In H. Winner, S. Hakuli, F. Lotz, & C. Singer (Eds.). *Handbook of Driver Assistance Systems* (pp. 19–33). Switzerland: Springer International Publishing. https://doi.org/10.1007/978-3-319-12352-3.
Dorf, R. C., & Bishop, R. H. (1995). *Modern control systems* (12th ed.). Reading, MA: Addison-Wesley.
Dozza, M., Schindler, R., Bianchi-Piccinini, G., & Karlsson, J. (2016). How do drivers overtake cyclists? *Accident Analysis and Prevention, 88*, 29–36. https://doi.org/10.1016/j.aap.2015.12.008.
Evans, N. J. (2019). A method, framework, and tutorial for efficiently simulating models of decision-making. *Behavior Research Methods, 1–15*. https://doi.org/10.3758/s13428-019-01219-z.
Farah, H., Piccinini, G. B., Itoh, M., & Dozza, M. (2019). Modelling overtaking strategy and lateral distance in car-to-cyclist overtaking on rural roads: A driving simulator experiment. *Transportation Research Part F: Traffic Psychology and Behaviour, 63*, 226–239. https://doi.org/10.1016/j.trf.2019.04.026.
Feng, F., Bao, S., Hampshire, R. C., & Delp, M. (2018). Drivers overtaking bicyclists-An examination using naturalistic driving data. *Accident Analysis and Prevention, 115*, 98–109. https://doi.org/10.1016/j.aap.2018.03.010.
Fisher, D. L., Pollatsek, A. P., & Pradhan, A. (2006). Can novice drivers be trained to scan for information that will reduce their likelihood of a crash?. *Injury Prevention, 12*, i25–i29. https://doi.org/10.1136/IP.2006.012021.
Fruttaldo, S., Piccinini, G., Pinotti, D., Tadei, R., & Perboli, G. (2012). Definition of a standard driver model. DESERVE D.3.1. Technical Report. EU. DESERVE. Deliverable D.3.1.
Gold, J. I., & Shadlen, M. N. (2001). Neural computations that underlie decisions about sensory stimuli. *Trends in Cognitive Sciences, 5*, 10–16. https://doi.org/10.1016/s1364-6613(00)01567-9.
Gold, J. I., & Shadlen, M. N. (2007). The neural basis of decision making. *Annual Review of Neuroscience, 30*, 535–574. https://doi.org/10.1146/annurev.neuro.29.051605.113038.
Gordon, T. J., & Magnuski, N. (2006). Modeling normal driving as a collision avoidance process. In *8th International Symposium, Advanced vehicle control; AVEC 06*. Hsinchu, Taiwan: National Tsing Hua University.
Gray, R., & Regan, D. M. (2005). Perceptual processes used by drivers during overtaking in a driving simulator. *Human Factors: The Journal of the Human Factors and Ergonomics Society, 47*, 394–417. https://doi.org/10.1518/0018720054679443.
Green, M. (2000). How Long Does It Take to Stop? Methodological Analysis of Driver Perception-Brake Times. *Transportation Human Factors, 2*, 195–216.
Hamdar, S. (2012). Driver behavior modeling. In A. Eskandarian (Ed.), *Handbook of intelligent vehicles* (pp. 537–558). Springer. https://doi.org/10.1007/978-0-85729-085-4.
Hastie, T., Tibsherani, R., & Freidman, J. (2009). *The elements of statistical learning* (2nd ed.). Springer. https://doi.org/10.1007/b94608.
Hildreth, E. C., Beusmans, J. M. H., Royden, C. S., & Boer, E. R. (2000). From vision to action: Experiments and models of steering control during driving. *Journal of Experimental Psychology. Human Perception and Performance, 26*, 1106–1132.
Hollnagel, E. (2006). A function-centred approach to joint driver-vehicle system design. *Cognition, Technology & Work, 8*, 169–173. https://doi.org/10.1007/s10111-006-0032-1.
Hosseini, S., Murgovski, N., de Campos, G. R., & Sjøberg, J. (2016). Adaptive forward collision warning algorithm for automotive applications. In *2016 American Control Conference (ACC)* (pp. 5982–5987).
Jagacinski, R. J., & Flach, J. M. (2002). *Control theory for humans: Quantitative approaches to modeling performance*. Publisher: Lawrence Erlbaum Associates, Inc.
Kiefer, R., Cassar, M., Flannagan, C., LeBlanc, D., Palmer, M., Deering, R., & Shulman, M. (2003). Forward Collision Warning Requirements Project: Refining the CAMP Crash Alert Timing Approach by Examining "Last-Second" Braking and Lane Change Maneuvers Under Various Kinematic Conditions. Technical Report January. National Highway Traffic Safety Administration, U.S. Department of Transportation. Washington, DC.
Kiefer, R. J., Leblanc, D. J., & Flannagan, C. A. (2005). Developing an inverse time-to-collision crash alert timing approach based on drivers' last-second braking and steering judgments. *Accident Analysis and Prevention, 37*, 295–303. https://doi.org/10.1016/j.aap.2004.09.003.
Kovaceva, J., Nero, G., Bärgman, J., & Dozza, M. (2018). Drivers overtaking cyclists in the real-world: Evidence from a naturalistic driving study. *Safety Science*. https://doi.org/10.1016/j.ssci.2018.08.022.
Kruschke, J. K. (2015). *Doing Bayesian data analysis*. Academic Press/Elsevier.
Lamble, D., Laakso, M., & Summala, H. (1999). Detection thresholds in car following situations and peripheral vision: Implications for positioning of visually demanding in-car displays. *Ergonomics, 42*, 807–815. https://doi.org/10.1080/001401399185306.
Lappi, O. (2014). Future path and tangent point models in the visual control of locomotion in curve driving. *Journal of Vision, 14*, 21. https://doi.org/10.1167/14.12.21.
Lee, D. N. (1976). A theory of visual control of braking based on information about time-to-collision. *Perception, 5*, 437–459. https://doi.org/10.1068/p050437, pMID: 1005020.
Lee, J. Y., & Lee, J. D. (2019). Modeling microstructure of drivers' task switching behavior. *Journal of Human Computer Studies, 125*, 104–117. https://doi.org/10.1016/j.ijhcs.2018.12.007.
Lehtonen, E., Lappi, O., & Summala, H. (2012). Anticipatory eye movements when approaching a curve on a rural road depend on working memory load. *Transportation Research Part F: Traffic Psychology and Behaviour, 15*, 369–377. https://doi.org/10.1016/j.trf.2011.08.007.
Levison, W., & Cramer, N. (1995). *Description of the integrated driver model (Technical report no. 7840)*. Cambridge, MA: Bolt, Berenak, & Newman Systems & Technologies.
Levulis, S. J., DeLucia, P. R., & Jupe, J. (2015). Effects of oncoming vehicle size on overtaking judgments. *Accident Analysis and Prevention, 82*, 163–170. https://doi.org/10.1016/j.aap.2015.05.024.

Lewis, F., & Syrmos, V. (1995). *Optimal control*. New York: Willey.
Llorca, C., Angel-Domenech, A., Agustin-Gomez, F., & Garcia, A. (2017). Motor vehicles overtaking cyclists on two-lane rural roads: Analysis on speed and lateral clearance. *Safety Science, 92*, 302–310. https://doi.org/10.1016/j.ssci.2015.11.005.
Maddox, M. E., & Kiefer, A. (2012). Looming threshold limits and their use in forensic practice. *Proceedings of the Human Factors and Ergonomics Society Annual Meeting, 56*, 700–704. https://doi.org/10.1177/1071181312561146.
Markkula, G. (2014). Modeling driver control behavior in both routine and near-accident driving. *Proceedings of the Human Factors and Ergonomics Society Annual Meeting, 58*, 879–883. https://doi.org/10.1177/1541931214581185.
Markkula, G. (2015). *Driver behavior models for evaluating automotive active safety: From neural dynamics to vehicle dynamics*. Chalmers University of Technology.
Markkula, G., Benderius, O., Wolff, K., & Wahde, M. (2012). A review of near-collision driver behavior models. *Human Factors, 54*, 1117–1143. https://doi.org/10.1177/0018720812448474, pMID: 23397819.
Markkula, G., Boer, E., Romano, R., & Merat, N. (2018). Sustained sensorimotor control as intermittent decisions about prediction errors: Computational framework and application to ground vehicle steering. *Biological Cybernetics, 112*, 181–207. https://doi.org/10.1007/s00422-017-0743-9.
Markkula, G., Engström, J., Lodin, J., Bärgman, J., & Victor, T. (2016). A farewell to brake reaction times? Kinematics-dependent brake response in naturalistic rear-end emergencies. *Accident Analysis and Prevention, 95*, 209–226. https://doi.org/10.1016/j.aap.2016.07.007.
Matson, T., & Forbes, T. (1938). Overtaking and passing requirements as determined from a moving vehicle. In *Proceedings of the Highway Research Board* (pp. 100–112).
McLaughlin, S. B., Hankey, J. M., & Dingus, T. A. (2008). A method for evaluating collision avoidance systems using naturalistic driving data. *Accident Analysis & Prevention, 40*, 8–16. https://doi.org/10.1016/J.AAP.2007.03.016.
Nashner, L. M., & Cordo, P. J. (2004). Relation of automatic postural responses and reaction-time voluntary movements of human leg muscles. *Experimental Brain Research, 43*, 395–405.
O'Dwyer, A. (2009). *Handbook of PI and PID Controller Tuning Rules* (3rd ed.). Imperial College Press. https://doi.org/10.1142/p575. https://www.worldscientific.com/worldscibooks/10.1142/p575.
Piccinini, G. B., Moretto, C., Zhou, H., & Itoh, M. (2018). Influence of oncoming traffic on drivers' overtaking of cyclists. *Transportation Research Part F: Traffic Psychology and Behaviour, 59*, 378–388. https://doi.org/10.1016/j.trf.2018.09.009.
Prokop, G. (2001). Modeling human vehicle driving by model predictive online optimization modeling. *Vehicle System Dynamics, 35*, 19–53. https://doi.org/10.1076/vesd.35.1.19.5614.
Rasch, A., Boda, C. N., Thalya, P., Aderum, T., Knauss, A., & Dozza, M. (2019). Drivers overtaking cyclists: How do the oncoming traffic and the position of the cyclist within the lane influence maneuvering? In *International Cycling Safety Conference, ICSC, Australia*. .
Ratcliff, R. (1978). A theory of memory retrieval. *Psychological Review, 85*, 59–108. https://doi.org/10.1037/0033-295X.85.2.59.
Ratcliff, R., & Smith, P. L. (2004). A Comparison of Sequential Sampling Models for Two-Choice Reaction Time. *Psychological Review, 111*, 333–367. https://doi.org/10.1037/0033-295X.111.2.333.
Ratcliff, R., Smith, P. L., Brown, S. D., & Gail, M. (2016). Diffusion decision model: Current issues and history. *Trends in Cognitive Sciences, 20*, 260–281. https://doi.org/10.1016/j.tics.2016.01.007.
Ratcliff, R., & Strayer, D. (2014). Modelling simple driving tasks with one-boundary diffusion model. *Psychonomic Bulletin & Review, 21*, 577–589. https://doi.org/10.3758/s13423-013-0541-x.
Rivera, D. E., Morari, M., & Skogestad, S. (1986). Internal model control: PID controller design. *Industrial & Engineering Chemistry Process Design and Development, 25*, 252–265. https://doi.org/10.1021/i200032a041. https://pubs.acs.org/doi/abs/10.1021/i200032a041.
Rogers, S., & Girolami, M. (2016). *A First Course in Machine Learning (Machine Learning and Pattern Recognition)* (2nd ed.). Chapman and Hall CRC.
Salvucci, D. D. (2006). Modeling driver behavior in a cognitive architecture. *Human Factors: The Journal of the Human Factors and Ergonomics Society, 48*, 362–380. https://doi.org/10.1518/001872006777724417.
Salvucci, D. D., & Gray, R. (2004). A two-point visual control model of steering. *Perception, 33*, 1233–1248. https://doi.org/10.1068/p5343.
Shackel, S. C., & Parkin, J. (2014). Influence of road markings, lane widths and driver behaviour on proximity and speed of vehicles overtaking cyclists. *Accident Analysis and Prevention, 73*, 100–108. https://doi.org/10.1016/j.aap.2014.08.015.
Sheridan, T., & Ferrell, W. (1981). *Man-machine systems, information, control and decision models of human performance*. Cambridge, MA: The MIT Press.
Shinar, D. (2017). *Traffic safety and human behavior* (2nd ed.). Emerald publishing limited.
Sjöberg, J., Coelingh, E., Ali, M., Brännström, M., & Falcone, P. (2010). Driver models to increase the potential of automotive active safety functions. In *2010 18th European Signal Processing Conference* (pp. 204–208).
Smith, M., Flach, J., Dittman, S., & Stanard, T. (2001). Monocular optical constraints on collision control. *Journal of Experimental Psychology: Human Perception and Performance, 27*, 395–410. https://doi.org/10.1037/0096-1523.27.2.395.
Summala, H. (2007). Towards understanding motivational and emotional factors in driver behaviour: Comfort through satisficing. In P. C. Cacciabue (Ed.), *Modelling driver behaviour in automotive environments*. London: Springer.
Summala, H., Lamble, D., & Laakso, M. (1998). Driving experience and perception of the lead car's braking when looking at in-car targets. *Accident Analysis and Prevention, 30*, 401–407. https://doi.org/10.1016/S0001-4575(98)00005-0.
Treiber, M., & Kesting, A. (2013). *Traffic flow dynamics*. Berlin, Heidelberg: Springer. https://doi.org/10.1007/978-3-642-32460-4.
Walker, I. (2007). Drivers overtaking bicyclists: Objective data on the effects of riding position, helmet use, vehicle type and apparent gender. *Accident Analysis and Prevention, 39*, 417–425. https://doi.org/10.1016/j.aap.2006.08.010.
Wann, J. P., & Wilkie, R. M. (2004). How do we control high speed steering? In L. Vaina, S. Beardsley, & S. Rushton (Eds.), *Optic flow and beyond. Synthese library, studies in epistemology, logic, methodology and philosophy of science* (pp. 401–419). Springer. https://doi.org/10.1007/978-1-4020-2092-6.
Wilson, T., & Best, W. (1982). Driving strategies in overtaking. *Accident Analysis and Prevention, 14*, 179–185. https://doi.org/10.1016/0001-4575(82)90026-4.
Winner, H., Hakuli, S., Lotz, F., & Singer, C. (2016). *Handbook of driver assistance systems*. Switzerland: Springer International Publishing. https://doi.org/10.1007/978-3-319-12352-3. <http://link.springer.com/10.1007/978-3-319-12352-3>.
Xue, Q., Markkula, G., Yan, X., & Merat, N. (2018). Using perceptual cues for brake response to a lead vehicle: Comparing threshold and accumulator models of visual looming. *Accident Analysis and Prevention, 118*, 114–124. https://doi.org/10.1016/j.aap.2018.06.006.
Yilmaz, E. H., & Warren, W. H. (1995). Visual control of braking: a test of the tau hypothesis. Journal of experimental psychology. *Human Perception and Performance, 21*, 996–1014.